

# THE THEORY OF AN ACTIVE MAGNETIC REGENERATIVE REFRIGERATOR\*

J. A. Barclay  
Los Alamos National Laboratory

## ABSTRACT

The adiabatic temperature change with field is limited to about 2 K/Tesla for ferromagnets near their Curie temperatures by the change of magnetization with temperature and the lattice heat capacity. Hence, practical magnetic refrigerators operate on a regenerative cycle such as the Brayton cycle. One way to execute this cycle is through the use of an active magnetic regenerator, i.e. a regenerator composed of magnetic material that is cycled in and out of a magnetic field with appropriate fluid flows. The theory of these devices can be predicted by solving the partial differential equations that describe fluid flow combined with heat transfer between the fluid and the magnetic solid. The active magnetic regenerator is described along with the method of calculation. Temperature profiles for a normal regenerator and a magnetic regenerative refrigerator are shown.

## INTRODUCTION

Many applications of advanced technology require low-temperature refrigeration for proper operation. Devices ranging from superconducting magnets and generators, infrared sensors, maser amplifiers to Josephson-junction computers and SQUID detectors all need a variety of refrigeration power at temperatures ranging from  $\sim 4$  K to  $\sim 60$  K. Each application puts a slightly different set of constraints on the refrigerator but some of the more desirable features are high reliability and long lifetime, small volume and mass, and, of course, high efficiency. Conventional gas-cycle refrigerators have been used for most present refrigeration needs but with the push for less massive, higher efficiency coolers, especially for some space missions, there is a necessity to explore new ways to obtain better refrigerators.

One promising method is magnetic refrigeration where the magnetocaloric effect is used in place of gas compression and expansion.<sup>(1-5)</sup> In contrast to regenerative gas-cycle stages, magnetic-refrigerator devices tend to perform best at low temperatures particularly from 4 K to 20 K

\*This work was performed under the auspices of the U.S. D.O.E. and support from D.O.E., DARPA, WPAFB, and NASA (K.S.C.) is gratefully acknowledged.

but may also perform well from ~20 K to ~77 K. In this paper, I describe the active magnetic regenerator concept that may be useful in practical designs in the 20 to 77 K range.

## THEORY

### MAGNETOCALORIC EFFECT

Above ~20 K ferromagnetic materials near their Curie temperature must be used to achieve the entropy change required for refrigeration of a load. Figure 1 shows calculated entropy-temperature curves for a typical ferromagnet with a Curie temperature of 40 K. Typical gas entropy changes are included for comparison. The entropy changes on this figure are calculated using the molecular field model for the magnetic equation of state<sup>(6)</sup> and the Debye-model for the heat capacity.<sup>(7)</sup> With these models the entropy changes as a function of temperature and magnetic field can be found according to

$$dS = \frac{C_B}{T} dT + \left( \frac{\partial M}{\partial T} \right)_B dB \quad . \quad (1)$$

The isothermal entropy changes or adiabatic temperature changes can be obtained from these curves. Figure 1 also shows that a single magnetic material can only span a limited temperature range, typically 20 to 40 K. Therefore, to span a temperature range from 20 K to 75 K, at least two or three different materials must be used. The materials can be in separate stages or combined in a single-stage active magnetic regenerator.

### MAGNETIC REGENERATOR

#### Descriptive Theory<sup>(4)</sup>

The active magnetic regenerator comprises several magnetic materials that are thermodynamically cycled to provide the refrigeration over an extended temperature range. The basic theory is that of an ordinary regenerator except that the temperature of the materials can be changed by the application or removal of a magnetic field and a displaced thermal wavefront propagates back and forth in the regenerator. The materials that might be used in a magnetic regenerator are gadolinium intermetallic compounds that are prepared by arc melting and are relatively cheap and stable to oxidation. In order to achieve excellent heat transfer, the material could be put into a chip geometry with an effective particle diameter of ~0.5 mm. Because the pressure drop across an efficient regenerator would have to be very small, typically  $10^4$ - $10^5$  Pa, there is no equivalent pressure wave problem as in normal regenerators dealing with compressed and expanded gas movement. This also should avoid the "dust" problem that comes from the continual pressure pulsing in ordinary Pb shot regenerators. Each material completes a small Brayton cycle near its Curie temperature, but when all the materials are combined, they yield

a Brayton cycle over an extended temperature range, e.g., 20-75 K. The basic cycle, illustrated in Fig. 2 is described below.

Consider a porous-bed regenerator composed of a series of different ferromagnetic materials with Curie temperature  $T_0$  gradually decreasing from the sink temperature  $T_H$  to the load temperature  $T_C - \Delta T_C$ , as shown in the top frame of Fig. 2. Also consider that the temperature gradient is uniform except for the constant temperatures at the ends of the regenerator, as shown in the second frame of Fig. 2. (For start up from a warm condition, i.e.,  $T_H$  everywhere, several cycles are also required to reach the condition assumed above, so for simplicity we start with an established temperature gradient.) Upon application of a magnetic field, the temperature along the bed adiabatically increases by  $\Delta T$ , which is about 15-20 K for a 10-T field, as shown in the third frame of Fig. 2. After the field is applied, helium or hydrogen gas, at temperature  $T_C$ , is pushed through the bed from the cold end, which is now at  $T_C$ . As the gas at  $T_C$  enters the bed, the gas warms as the bed cools and a thermal wavefront of magnitude  $T_H + \Delta T_H - T_C$  is established, as shown in the fourth frame of Fig. 2. The overall wavefront propagates through the regenerator (to the right in the fourth frame of Fig. 2) as gas continues to flow into the bed at  $T_C$ . The gas leaves the regenerator at  $T_H + \Delta T_H$  until the thermal wavefront arrives at the end of the regenerator. When this happens, the gas flow stops and the regenerator is adiabatically demagnetized. The temperatures all along the bed drop by  $\Delta T$ , as shown in frame 5 of Fig. 2, in preparation for the reverse flow of gas. The gas that came out of the regenerator at  $T_H + \Delta T_H$  during the magnetized stage is put through a heat exchanger and cooled to  $T_H$  before it is pushed back into the regenerator after demagnetization. Another thermal wave of magnitude  $T_H - T_C + \Delta T_C$  is established, but it travels in the opposite direction to the first thermal wavefront, as shown in the bottom frame of Fig. 2. The gas exits the cold end at  $T_C - \Delta T_C$  and is heated when it contacts a load at  $T_C$ . When the thermal wave reaches the cold end of the regenerator, the gas flow stops and the cycle now repeats as the regenerator is again magnetized. This concept can be incorporated into both reciprocating and wheel modes. In both modes, the rate of magnetization and demagnetization is limited in practice to  $<1$  Hz by the heat transfer coefficients. If the heat transfer could be improved, the frequency could be increased but eventually the eddy current power would become significant; probably near 5-10 Hz. If the eddy current and heat transfer problems could be eliminated, the upper limit on cycle frequency is given by the spin-lattice relaxation rate; typically to  $\sim 1$  kHz for gadolinium compounds.

The efficiency of the active magnetic regenerative refrigerator is potentially quite high for several reasons. The basic process, magnetization/demagnetization, is inherently highly reversible compared to the compression/expansion of a gas. The work for the cycle can be put in via a  $\sim 90\%$  efficient motor rather than through a 60-70% efficient compressor as in a gas cycle. The external heat exchanger and other losses are comparable in the gas and magnetic systems. In the magnetic system the heat transfer during the regenerative stages will be the dominant

inefficiency, thereby requiring excellent regenerator design with respect to heat transfer, viscous flow dissipation, and longitudinal conduction. If the regenerator can be made highly effective, the overall magnetic refrigerator efficiency can approach 50-60% of Carnot efficiency. This would be significantly higher than existing gas refrigerators such as Stirling-cycle devices.

### Mathematical Theory

The basic theory of thermal wavefront propagation through a porous bed was first presented approximately fifty years ago.<sup>(8)</sup> The temperature span across the bed was considered small enough so that the bed and gas properties could be taken as constant. Also, momentum and mass-continuity effects were ignored leaving only a set of energy-balanced equations to describe the problem. The one-dimensional, partial differential energy equations are

$$\text{fluid: } \alpha \rho_f C_f \frac{\partial T}{\partial t} = -\dot{m}_f C_f \frac{\partial T}{\partial x} + ha(\theta - T) \quad (2)$$

$$\text{solid: } (1 - \alpha) \rho_s C_s \frac{\partial \theta}{\partial t} = ha(T - \theta) + (1 - \alpha) \lambda_s \frac{\partial^2 \theta}{\partial x^2} \quad (3)$$

where  $\alpha$  is the porosity,  $\rho_f$ ,  $\rho_s$  are the fluid and solid densities, respectively,  $C_f$ ,  $C_s$  are the fluid and solid heat capacities, respectively,  $\dot{m}_f$  is the fluid mass flow rate,  $T$  is the fluid temperature,  $h$  is the conductance between the fluid and solid,  $\theta$  is the solid temperature,  $a$  is the contact area per unit volume of the bed, and  $\lambda_s$  is the effective axial thermal conductivity of the bed. When Eqs. (2) and (3) are numerically solved by finite difference techniques, they give a thermal wavefront propagating as a function of time.

For the prediction of the thermal-wavefront propagation in a regenerator with a large temperature gradient when all properties are temperature dependent, the one-dimensional equations for a porous bed are given by<sup>(9)</sup>

$$\frac{\partial \rho'}{\partial t} + \frac{\partial \rho' u}{\partial x} = 0 \quad (4)$$

$$\frac{\partial \rho' u}{\partial t} + \frac{\partial (\rho' u^2)}{\partial x} + \alpha \frac{\partial P}{\partial x} - \rho' g + \frac{f \rho (1 - \alpha) |u| u}{d_p} = 0 \quad (5)$$

$$\frac{\partial \rho' U}{\partial t} + \frac{\partial \rho' u U}{\partial t} + P \frac{\partial (\alpha u)}{\partial x} + \frac{6(1-\alpha)h}{d_p} (T - \theta) + \frac{4\alpha h'}{d_i} (T - \psi) - \frac{f \rho (1-\alpha) |u| u^2}{d_p} - \frac{\partial}{\partial x} (k_f \alpha \nabla T) = 0 \quad (6)$$

$$\rho'_s \frac{\partial U_s}{\partial t} - E_s - \frac{6(1-\alpha)h}{d_p} (T - \theta) - \frac{4(1-\alpha)h''}{d_i} (\psi - \theta) - \nabla \cdot [k_s (1-\alpha) \nabla \theta] = 0 \quad (7)$$

$$\rho'_w \frac{\partial U_w}{\partial t} - E_w + \frac{4(1-\alpha)d_i}{(d_o^2 - d_i^2)} h'' (\psi - \theta) - \frac{4d_i \alpha h'}{(d_o^2 - d_i^2)} (T - \psi) - \nabla \cdot (k_w \nabla \psi) = 0 \quad (8)$$

where  $\rho'$  is the effective fluid density,  $u$  is the velocity,  $P$  is the pressure,  $f$  is the friction factor,  $g$  is the gravitational constant,  $k_f$ ,  $k_s$ , and  $k_w$  are the thermal conductivities of the fluid, magnetic solid, and wall, respectively,  $\psi$  is the wall temperature,  $h'$  and  $h''$  are the fluid to wall and solid to wall conductance, respectively,  $d_i$  and  $d_o$  are the inner and outer diameters of the regenerator container, respectively,  $U$  is the internal energy, and  $E_s$  and  $E_w$  are heat sources or sinks such as eddy currents, heat leak from surrounding, and magnetocaloric effect.

## RESULTS

The coupled non-linear, partial differential equations that describe the one-dimensional processes in the porous magnetic bed can be solved only by numerical techniques. Equations (4) through (8) have been solved by using the finite difference method. As a model a stainless steel container 0.05 m inner diameter by 0.0025 m (.010") wall and 0.05 m long was chosen. The container was filled with lead spheres with a 0.0005 m (0.5mm) diameter to a porosity of 40%. For the calculations described here the initial conditions of the bed were stationary helium gas at 25 K and 1.013 MPa. To establish a thermal gradient across the bed, a pressure increase of 0.03 MPa was introduced suddenly on the right end of the bed where the input gas temperature was fixed at 75K. A thermal wavefront propagated across the bed until the temperature on the left end of the bed started to rise slightly above 25 K. At that point the pressure difference was reversed and the inlet gas temperature on the left was fixed at 25 K. The net mass flow per cycle was constrained to be zero. Figure 3 shows the

gas, lead spheres, and wall temperature profiles as a function of distance across the bed after several complete cycles of gas flow reversal. The solid temperature profile is characteristic of a regenerator where the bed-material heat capacity decreases as a function of temperature.

The behavior of a magnetic regenerator was calculated by using the same model as previous except that now it was assumed that the bed was composed of a series of magnetic materials whose combined adiabatic temperature change upon magnetization or demagnetization was a uniform 10 K across the entire bed. The magnetic regenerator cycle was started from a normal regenerator profile between 25 and 75 K. The magnetic material temperature was then increasing rapidly by 10 K after which gas was introduced from the left at 35 K. The gas exited the right end of the bed at between  $\sim$ 85 and 80 K. After an arbitrary mass flux such that the outlet temperature started to drop, the pressure difference was removed and the magnetic material demagnetized everywhere by 10 K. Upon completion of the demagnetization the flow was reversed with the temperature of the inlet gas fixed at 75 K. The exiting gas on the left end of the bed was between  $\sim$ 25 and 28 K. When the net mass flow at the left end of the bed was zero, the cycle was repeated. Figure 4 illustrates the temperature profiles at various stages of the cycle after approximately ten cycles.

#### DISCUSSION AND CONCLUSIONS

There are many interesting observations that come from these calculations but I will only mention a few. The effect of the variation in heat capacity as a function of temperature is very obvious during magnetization or demagnetization because the wall to solid temperature difference remains larger longer at the higher-temperature end of the regenerator. The choice of a thin container wall reduces the shuttle effect in this model but with thicker walls more distinct influence would be apparent. A second obvious effect is the longitudinal conduction in the bed. The solid temperature at either end of the regenerator tends to be a degree or two from the corresponding gas inlet temperature. With a 35 to 75 K temperature difference across the bed, a slightly longer bed would probably be a better choice.

Another observation was that after the pressure difference across the bed was removed, during magnetization or demagnetization, the gas undergoes substantial movement due to temperature gradients. This gas movement has very little effect in this temperature range because the thermal mass of the gas is small compared to the solid. However, in the 4-10 K temperature range where helium has a larger volumetric-heat-capacity than most materials, the effects of moving helium could be significant.

The calculations described in this work indicate that a magnetic regenerator can be cycled successfully to provide cold gas for refrigeration between 25 and 35 K. The exhaust gas can be used to reject heat between 85 and 75 K. Many questions about a detailed magnetic regenerative refrigerator design remain unanswered at this time but calculations of the kind described in this paper should help obtain a successful design.

- Q1. Yes. In both the reciprocating and wheel modes there is a definite requirement for force compensation as the magnetic material is moved into and out of the magnetic field. At 9T with 1 liter of gadolinium, the forces are in the many ton range.
- Q2. Yes, we have looked at staging of the refrigerator so the maximum amount of heat leak is intercepted at the highest possible temperature. This is clearly required to obtain high efficiency.
- Q3. The source of field is a superconducting magnet. The best way to incorporate a superconducting magnet into a refrigerator is to put the magnet in persistent mode once it is charged and to leave it alone. Cycling the magnet requires careful attention to an energy storage device at room temperature and is definitely not recommended on the first designs.
- Q4. Very small pressure ratios are used because the porous bed has only a small pressure drop if it is highly efficient. The cycle time for the gas in a typical AMR is about 0.1 to 1 Hz. The pressure ratio has to be different at the cold end and hot end of the regenerator to have mass conservation for a complete cycle.

#### ACKNOWLEDGEMENTS

It is a pleasure to thank Frank Harlow for several hours of discussion on the problems of finite-difference methods.

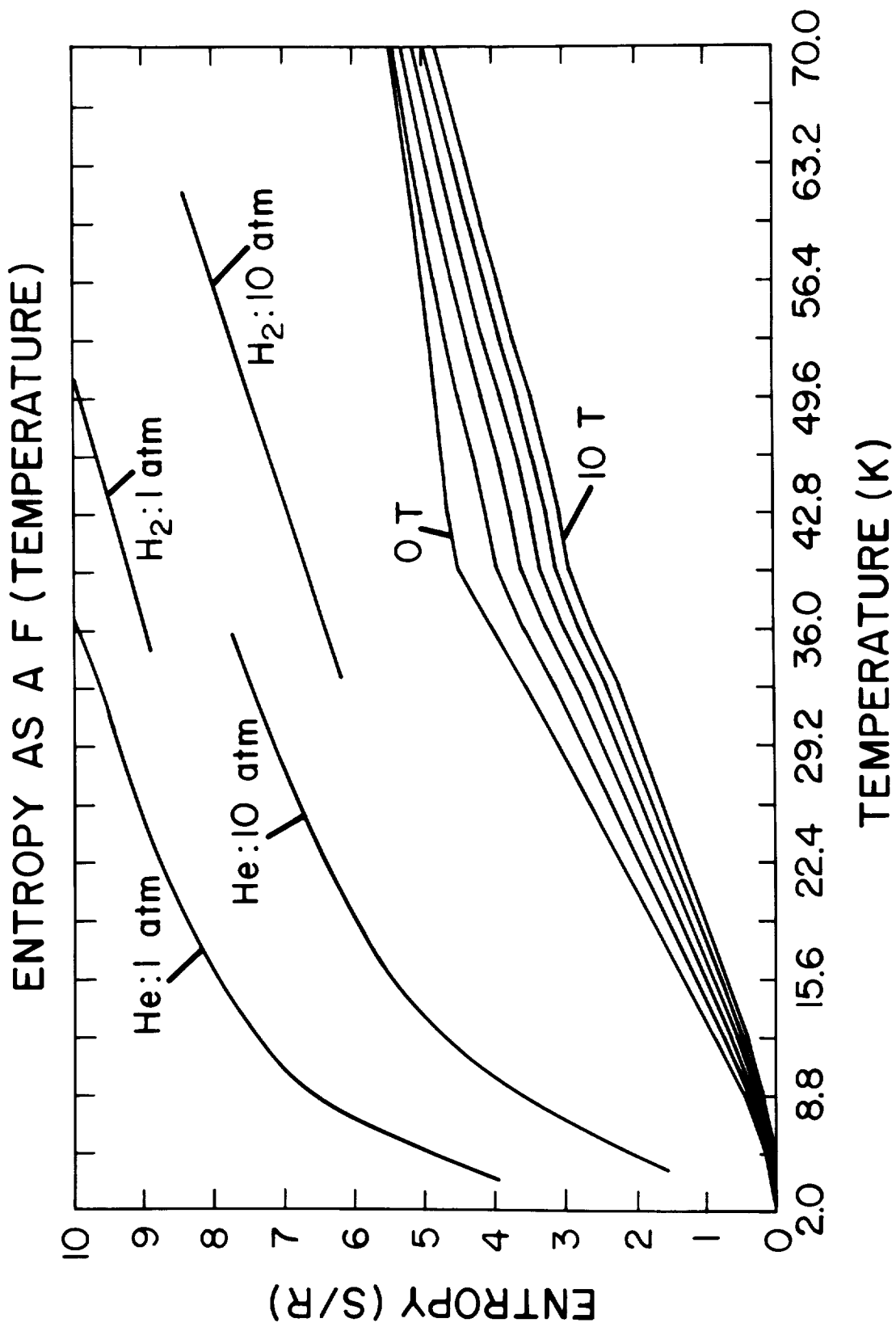


Figure 1. Calculated Entropy-Temperature curves for a typical ferromagnetic with a Curie temperature of 40 K. The curves for the helium and hydrogen gas are added for comparison.

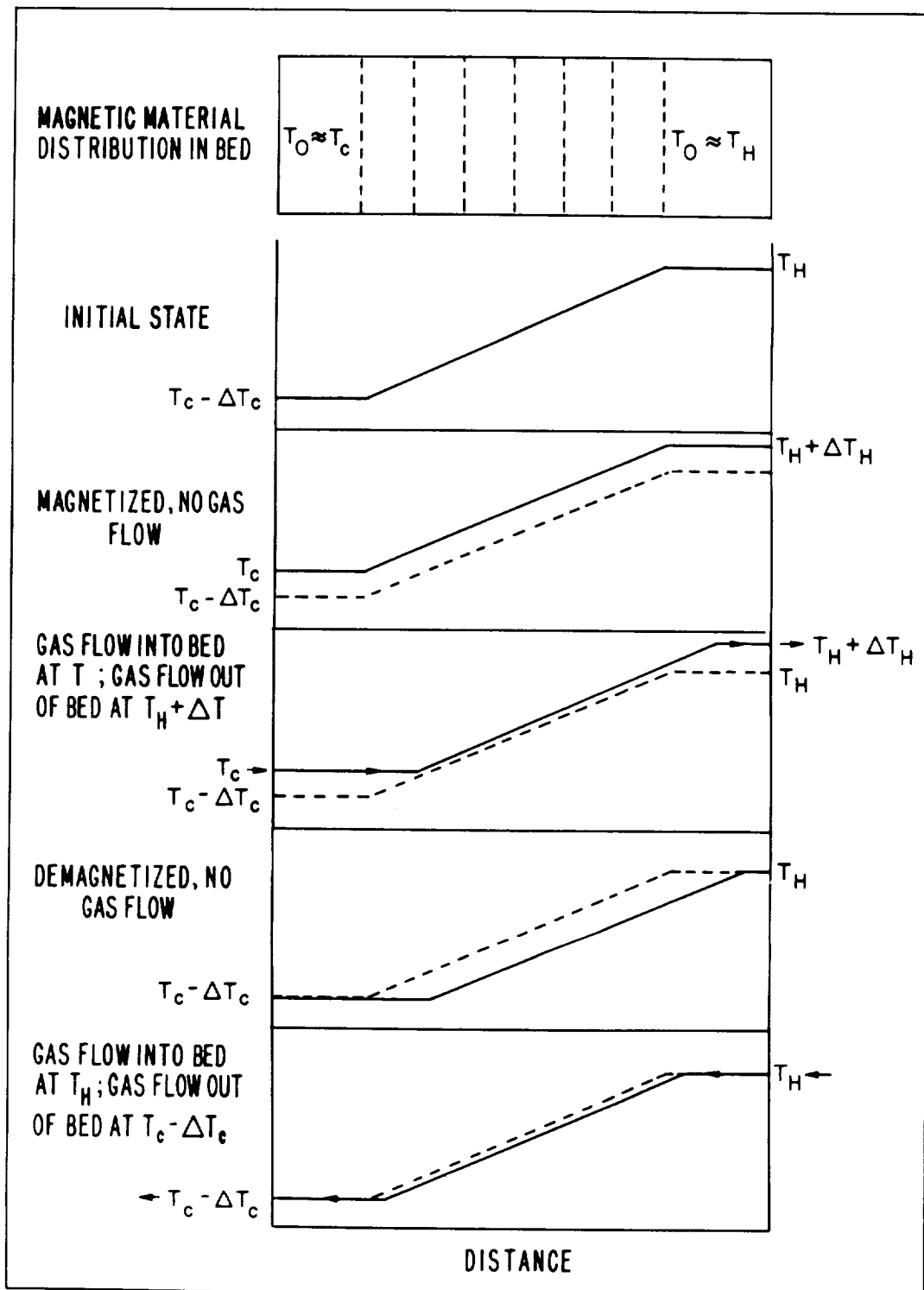


Figure 2. A schematic of the various parts of an active magnetic regenerative refrigeration cycle.

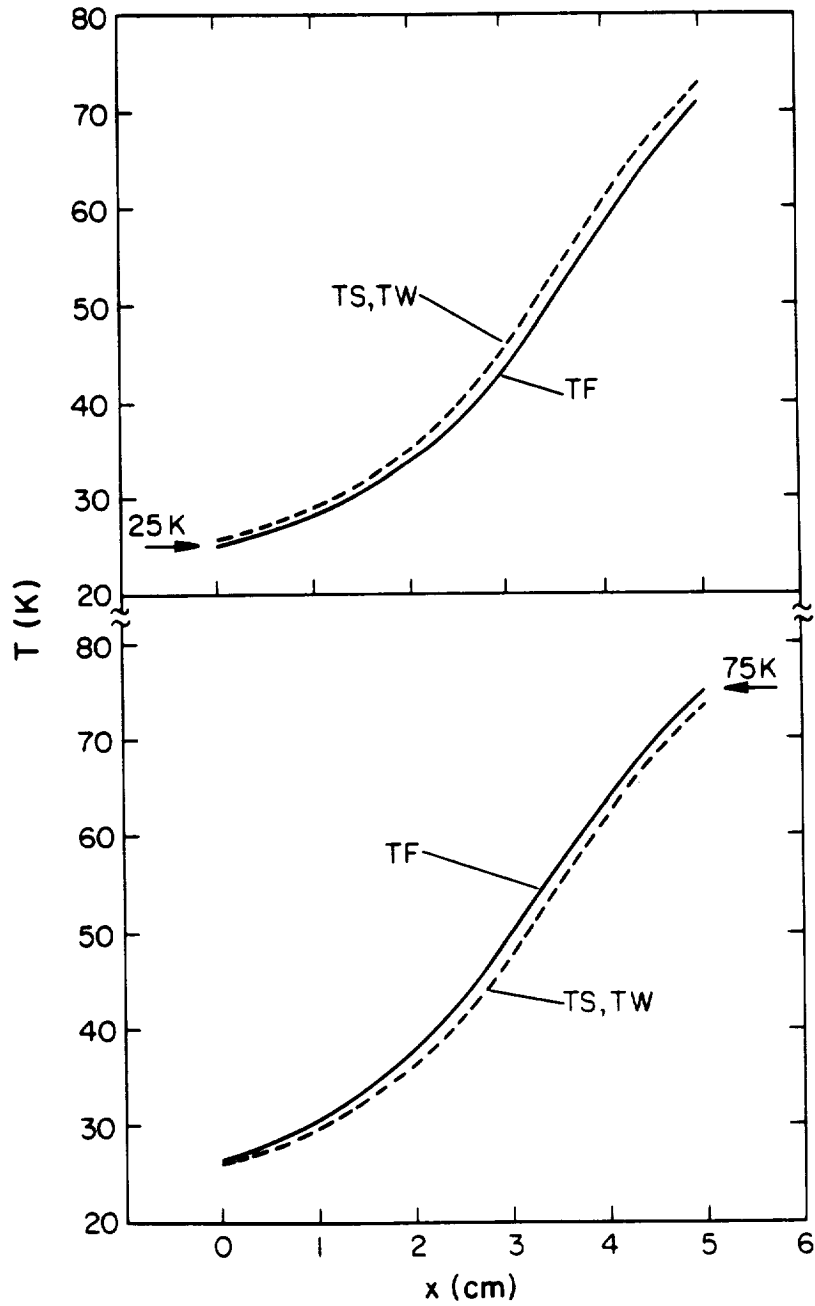


Figure 3. The temperature profiles of the gas, solid, and wall as a function of distance in a ordinary regenerator after cycling between 25 and 75 K.

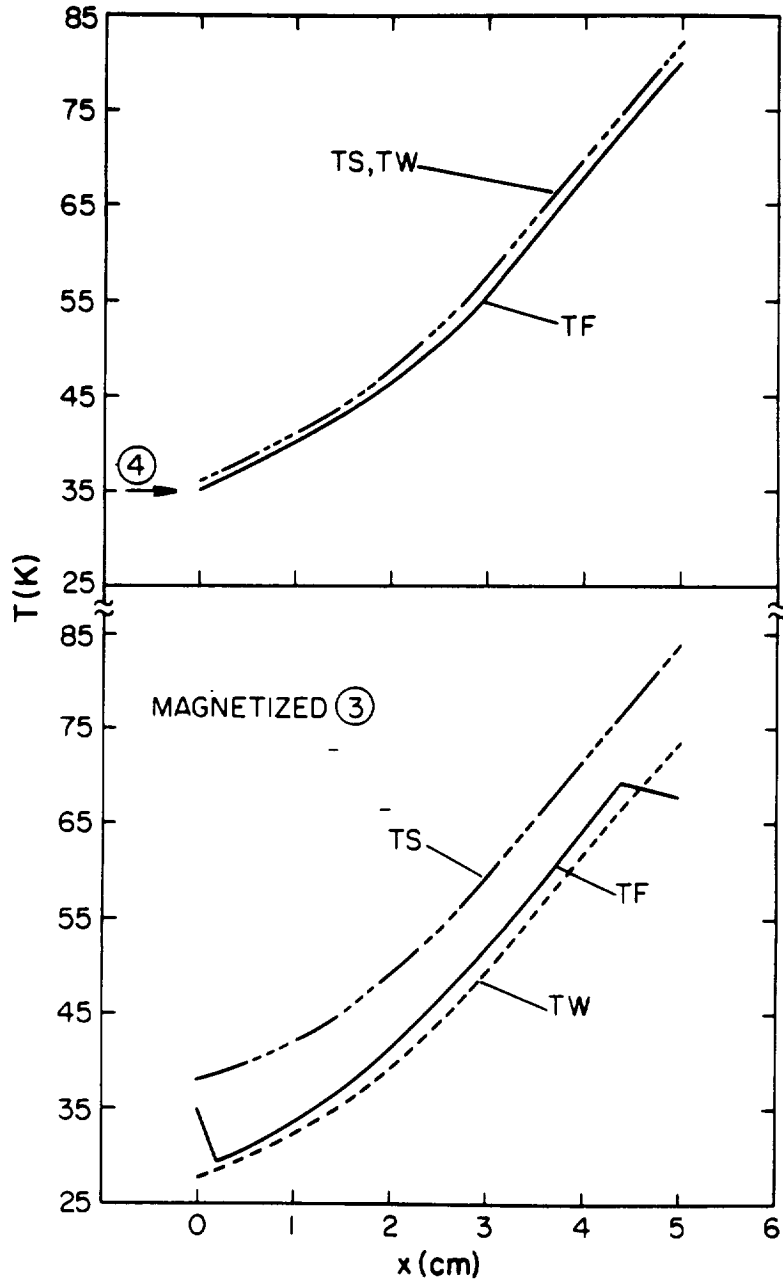


Figure 4. The temperature profiles of the gas, magnetic solid, and wall as a function of distance in a magnetic regenerator. Frame 3 indicates temperatures after magnetization and frame 4 after gas flow from the left end.

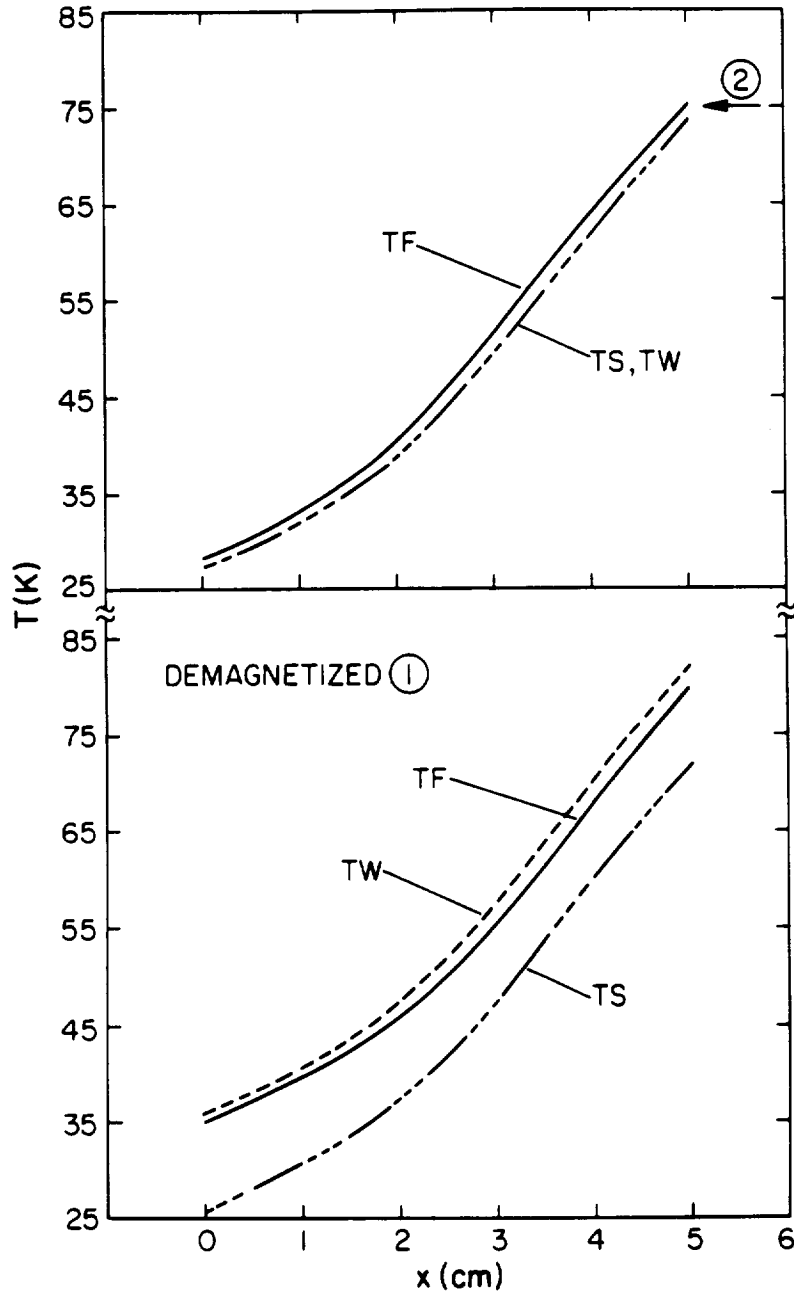


Figure 5. The temperature profiles of the gas, magnetic solid, and wall as a function of distance in a magnetic regenerator. Frame 1 indicates temperatures after demagnetization and frame 2 after gas flow from the right end.

## REFERENCES

1. J. R. van Geuns, "A Study of a New Magnetic Refrigerating Cycle," Philips Res. Rep. Suppl. 6 (1966).
2. G. V. Brown, "A Magnetic Heat Pump Near Room Temperature," J. Appl. Phys. 47, 3673 (1976).
3. W. A. Steyert, "Stirling Cycle Rotating Magnetic Refrigerators and Heat Engines for use near Room Temperature," J. Appl. Phys. 49, 1216 (1978).
4. J. A. Barclay, "Can Magnetic Refrigerators Liquefy Hydrogen at High Efficiency?," Trans. Am. Soc. Mech. Eng. 1981, paper 81-HT-82.
5. T. Hashimoto, T. Numasawa, M. Shino, and T. Okada, "Magnetic Refrigeration in the temperature range from 10 K to room temperature: the Ferromagnetic refrigerants," Cryogenics 21, 647 (1981).
6. J. S. Smart, Effective Field Theories of Magnetism (W. B. Saunders Co., Philadelphia, 1966) Chp. 3.
7. C. Kittel, Introduction to Solid State Physics (John Wiley and Sons, Inc., New York, 5th ed., 1976), Chp. 5.
8. T. E. W. Schumann, "Heat Transfer, A Liquid Flowing through a Porous Prism," J. Franklin Inst. 208, 405 (1929).
9. F. H. Harlow and A. A. Amsden, "Numerical Calculation of Multiphase Fluid Flow," J. Comput. Phys. 17, 19 (1975).